EQA - International Journal of Environmental Quality
ISSN 2281-4485 - Vol. 62 (2024): 45-54
Journal homepage: https://eqa.unibo.it/

published by

Low-temperature desulfurization forecasting using soft computing models

Robert Someo Makomere[1*], Hilary Rutto[1], Alfayo Alugongo[2], Lawrence Koech[1]

[1] Clean Technology and Applied Materials Research Group, Department of Chemical and Metallurgical Engineering, Vaal University of Technology, Vanderbijlpark, Gauteng, South Africa
[2] Department of Industrial Engineering, Operations Management, and Mechanical Engineering, Vaal University of Technology, Vanderbijlpark, Gauteng, South Africa

* Corresponding author E-mail: 220178178@edu.vut.ac.za

Article info
Received 3/2/2024; received in revised form 14/5/2024; accepted 15/6/2024
DOI: 10.6092/issn.2281-4485/19040

Abstract
Flue Gas Desulfurization (FGD) is pivotal in reducing Sulfur Dioxide (SO_2) concentrations through neutralization. This study explored dry FGD modeling using Artificial Neural Networks (ANN) and Adaptive Neuro-Fuzzy Inference Systems (ANFIS). The independent parameters used were diatomite to $Ca(OH)_2$ ratio, hydration time, hydration temperature, SO_2 concentration, and sulfation temperature, while the output responses incorporated were sulfation efficiency (Y_1) and sorbent conversion (Y_2). ANN simulations employed the Levenberg-Marquardt (LM), Bayesian Regularization (BR), and Scaled Conjugate Gradient (SCG) algorithms with 7 to 10 hidden cells. The sigmoid and linear functions served as trigger mechanisms. ANFIS models, utilizing grid partitioning and subtractive clustering, were trained with hybrid and backpropagation methods. Seven ANFIS membership functions were compared for the best-fit model. The computing models were critiqued using RMSE, MSE, and R^2 statistical metrics. Numerical error analysis favored the ANN program, with BR exhibiting the highest R^2 values (0.9987 for Y_1, 0.9986 for Y_2). However, the SCG algorithm emerged as the most dependable model due to its lowest RMSE and MSE values. In contrast, the ANFIS model demonstrated inferior R^2 values and forecasting capabilities. This investigation provided nuanced insights into dry FGD modeling, elucidating the interplay between computational methodologies and process parameters.

Keywords
Deep learning, desulfurization, neural networks, fuzzy logic systems, emission control

Introduction

The presence of SO_2 in the atmosphere can cause a significant shift in the climate, with episodes of rapid cooling spanning years or global warming following high gas releases. Coal-fired power facilities are primary anthropogenic sources of air pollution. Sulfur dioxide, one of the criteria pollutants, contributes to human health problems, such as asthma and heart attacks (Manisalidis et al. 2020; Heaviside et al. 2021). A considerable quantity of this gas reduces the ability of the atmosphere to filter itself owing to the reduced. concentration of the hydroxide radical (OH), which is used to convert SO_2 to sulfuric acid. This translates to elevated levels of other gas pollutants and the formation of acid rain (Fatima et al. 2020). Dry flue gas desulfurization (DFGD) is a retrofit SO2 capture system that can be easily integrated by power plants with no emission control technologies (Carpenter 2012; Li et al. 2022). Scaling laboratory experiments to pilot plants or fully operational units necessitates a profound comprehension of the desired outcomes, including scrubbing efficiencies and reagent.

EQA 62 (2024): 45-54

DOI: 10.6092/issn.2281-4485/19040

conversion. Mathematical computations, such as computational fluid dynamics (CFD), have been immensely leveraged in modeling studies to optimize reaction variables in the neutralization process. (Tryggvason 2016; Bhatti et al. 2020; Lerotholi et al. 2022). Soft computing technologies can be employed as alternate techniques for prediction processes in desulfurization units. Artificial neural networks (ANN) are software systems composed of layered structures (input, hidden, and output layers) designed to mimic the learning and comprehension abilities of the human brain. (Roy et al. 2021; Jakšić et al. 2023). Mathematical equations and algorithms are used to analyze the relationship between data sets and generate accurate models and forecasted results. Each algorithm offers distinct benefits in terms of system memory and training time. The predicted data is evaluated by assessing errors and regression values to validate the correlation between atomic data and the synthetic values. An adaptive neuro-fuzzy inference system (ANFIS) is a hybrid method that syndicates the programming platforms of neural networks (NN) and fuzzy inference systems (FIS). The prediction capability of the system is achieved through thorough training of the ANN and the logical reasoning ability of the FIS (Chopra et al. 2021). This symbiotic networking reduces forecasting errors by optimizing hidden layer identification, a problem associated with ANN during metadata transmission. The backpropagation algorithm and the least squares approach are employed in the coding of input data. This system is subject to a set of IF-THEN rules developed by Takagi and Sugeno (TSK), each assigned a membership function (MF).

This work aimed to model and analyze dry flue gas desulfurization utilizing ANN and ANFIS. The performance of both simulation techniques was assessed and contrasted in terms of statistically significant non-linear error functions that measure the error distribution. However, most dry flue gas desulfurization research focuses on the one-factor-at-a-time procedure (OFAT). This experimental design requires a long time to evaluate. It cannot be used to predict the desired optimal adsorption efficiency as a series of contact between process variables. To the best of the authors' knowledge, there has been no comparative investigation on dry flue gas desulfurization using complex modeling methods such as FIS and NN. There is a dearth of literature on machine learning applications in the DFGD process,. as most researchers have focused on mature wet and semi-dry technologies (Guo et al. 2019; Fu et al. 2019; Kong et al. 2020). Consequently, our study is focused on bridging this disparity.

Materials and methods

Data mining

The data modeled in this study was gathered from a prior research analysis conducted on a fixed-bed desulfurization system (Figure 1) using an activated $Ca(OH)_2$-diatomite sorbent. (Makomere et al. 2023c). The experimental design utilized a central composite design from the Design-Expert v13.0.5.0 program, creating 50 datasets. The input variables (Table 1) were divided into five coded elements based on a star point distance of α=2 (alpha level 2). The factors considered entail the diatomite to $Ca(OH)_2$ ratio (A), the hydration time (B), the hydration temperature (C), the inlet SO_2 concentration (D), and the sulfation temperature (E). The output responses involved in assessing the impact of each input parameter were sulfation efficiency (Y_1) and reagent conversion (Y_2). The sulfation process that occurred, equation [1], can be described as an irreversible ion-exchange reaction involving the acidic SO_2 gas and the alkaline $Ca(OH)_2$ sorbent. The consumed sorbent was transformed into a dry salt, primarily made up of calcium sulfite ($CaSO_3$). The effluent gas was analyzed using a Testo-340 combustion flue gas analyzer and discarded through a fume chamber. The percentage reagent utilization (Y_2) can be calculated quantitatively using the SO_2 removal efficiency (Y_1) as shown in equations [1] , [2] and [3].

$$Ca\,(OH)_{2(s)} + SO_{2(g)} \rightarrow CaSO_{3(s)} + H2O_{(g)} \qquad [1]$$

$$\eta^{desox}\,(\%) = \left(1 - \frac{C_{out}}{C_{in}}\right) \times 100 \qquad [2]$$

$$\eta^{Ca} = \eta^{desox} * \frac{S}{Ca} \qquad [3]$$

where $\eta^{desox}(\%)$ is the percentage sulfur removal efficiency, C_{out} represents the outlet SO_2 concentration, C_{in} is the feed SO_2 concentration, η^{Ca} is the amount of calcium utilized, S and Ca are the molar quantities of sulfur and calcium, respectively (Makomere et al., 2023c).

EQA 62 (2024): 45-54

DOI: 10.6092/issn.2281-4485/19040

The input data was pre-processed using the min-max linear transformation, which scales the values to a range of 0 to 1, as shown in equation [4]. This process is crucial for creating dimensionless input variables that have reduced noise and outliers caused by variations in magnitude.

This necessitates the execution of optimal training for the ANN. The synthetic data was denormalized, equation [5], for comparison with the actual value.

$$z_i = \frac{[x_i - min\ (x)]}{[max\ (x)\ -\ min\ (x)]} \quad [4]$$

$$x_i = [z_i * (max - min)] \quad [5]$$

where z_i represents the normalized i[th] value, x_i is the i[th] value in the input data, $min(x)$ is the lowest value and $max(x)$ is the maximum value in the dataset (Eesa and Arabo 2017; Makomere et al., 2023a).

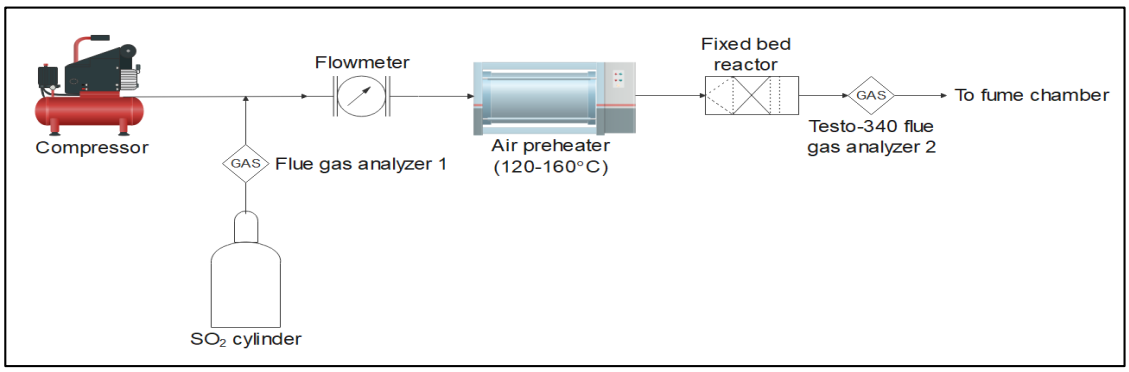

Figure 1 *Experimental setup*

Code	Experimental variable	Range
	Inputs	
A	Diatomite to $Ca(OH)_2$	0-1
B	Hydration time (hours)	3-7
C	Hydration temperature (°C)	50-90
D	Inlet SO_2 concentration (ppm)	500-2500-
E	Sulfation temperature (°C)	120-160
	Responses	
Y_1	SO_2 removal (%)	5-54
Y_2	Reagent conversion (%)	4-42

Table 1. *The scope of feed data used in ANN and ANFIS models.*

Artificial neural network (ANN) framework

The fitting tool (nftool) was executed in MATLAB R2023a to perform simulations using either the Levenberg-Marquardt (LMANN), Bayesian Regularization (BRANN), and Scaled Conjugate Gradient (SCGANN) backpropagation algorithms. For comparison purposes, each algorithm utilized an ANN design consisting of 5 input cells, 7 to 10 hidden cells, and 2 output cells (Figure 2). The selected database (Table 1) was divided into training (30), validation (10), and testing (10) using the divide-rand ANN function. The feedforward process involved transmitting information to the hidden layer after the input nodes were activated. This allowed for the computation of a potential correlation between the input and response parameters. Nonlinear (tansig and logsig) and linear (purelin) trigger functions were compared as hidden layer activators. The total output was recalibrated through synaptic weight mutation to minimize the distance between the experimental and the predicted ANN values (backpropagation). This process transcends to training termination when sufficient generalization is attained. Occasional initializing and reverting of the weights post-training were attempted to optimize output results. Retraining the network was limited to ten actions as it was discovered that the network performed poorly afterward.

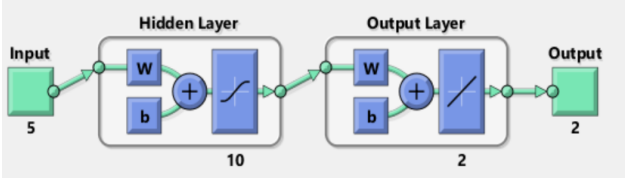

Figure 2. *A sample 5-10-2 ANN architecture.*

Adaptive neuro-fuzzy inference system (ANFIS) design

The fuzzy logic designer was also developed using the

EQA 62 (2024): 45-54

DOI: 10.6092/issn.2281-4485/19040

MATLAB R2023a program. The ANFIS prompt (>>fuzzy) was computed on the MATLAB window to initiate the Sugeno-type fuzzy inference system (FIS). Five input variables were used as feed data, and only one output variable was selected for model evaluation at a time (Figure 3). The information was sectioned into training (35) and testing (15) for programming. Input membership functions used to translate the input variables were triangular (trimf), trapezoidal (trapmf), generalized bell-shaped (gbellmf), Gaussian (gaussmf), Gaussian combination (gauss2mf), pi-shaped (pimf), and the difference between two sigmoidal (dsigmf) functions. The constant type of MF analyzed the target responses when generating the network. The hybrid and backpropagation algorithms were compared as optimization methods at 100 dataset passes at a given time (epochs). The system error was set to converge near zero. The network output was examined by utilizing the training and testing loss function (RMSE) to assess the level of concordance between the observed and predicted data. To generate the FIS model, grid partitioning-GP (genfis1) and subtractive clustering-SC (genfis2) were reviewed for correlation preeminence. The genfis2 model was established at a 0.5 range of influence, a squash factor of 1.25, an accept ratio of 0.5, and a reject ratio of 0.15. The >>evalfis (Output, dataOutput) code was utilized to generate projected data points for comparison with the ANN and empirical values.

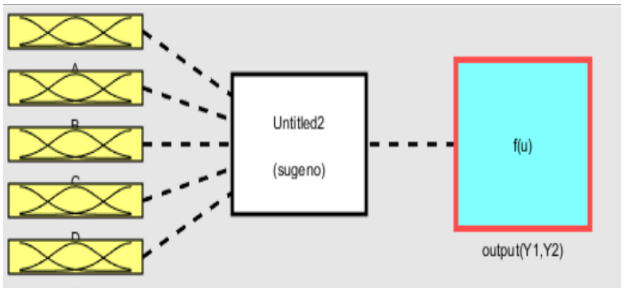

Figure 3. *Generic Sugeno FIS layout*

Model analysis

The evaluation of the ANN and ANFIS outcomes to determine the model with better performance relied on a high coefficient of determination (R^2) value, as well as lower values for root mean square error (RMSE) and mean square error (MSE). R^2 quantifies the degree of association between the developed model and the dependent variable using a scale ranging from 0 to 100% (Chicco et al. 2021). It is numerically expressed as shown in equation [6].

$$R^2 = \frac{\sum_{i=1}^{N}(D_p - D_e)}{\sum_{i=1}^{N}(D_p - D_{e_m})^2} \quad [6]$$

The RMSE and MSE statistical methods serve to perform data evaluation. In soft computing, MSE acts as a loss function indicator to quantify the effectiveness of a training algorithm and detect outliers (Badillo et al. 2020). The squared region ensures a detailed error calculation by adding more weight to these values. Small numbers indicate minimal disparity between the model data and the actual data, therefore allowing for the model to be applied in other domains. The RMSE is a square root of the MSE and is used to assess the suitability of a model for future trend analysis (Chai and Draxler 2014; Makomere et al. 2023b). RMSE and MSE can be calculated as defined in equations [7] and [8], respectively (Septiarini and Musikasuwan 2018).

$$RMSE = \sqrt{\frac{1}{N}\sum_{i=1}^{N}(D_e - D_p)^2} \quad [7]$$

$$MSE = \frac{1}{N}\sum_{i=1}^{N}(D_e - D_p)^2 \quad [8]$$

where N is the CCD experimental runs, D_{e_m} represents the average mean of the actual data, D_p is the predicted value and D_e is the actual value.

Results and discussion

Neural Network performance evaluation

From Figures 4a to 6a, training performance revolves around the comprehensive 'all' R^2 values. Notably, the BR script slightly outperforms LM and SCG, achieving a correlation coefficient square of 0.9973. This superiority is ascribed to the strategic adaptability of the BR programming to haphazard data, mitigating network overfitting (Jazayeri et al. 2016). Validation checks were absent (Figure 5) in the BRANN algorithm, thereby maximizing data for training activities. The LM tool secured the second position with an R^2 of 0.98491, while SCG exhibited the lowest value of 0.9761. Both LM and SCG scripts implement validation checks to curb overfitting. The SCG algorithm consistently produces lower MSE values

EQA 62 (2024): 45-54

DOI: 10.6092/issn.2281-4485/19040

than BR and LM, contributing to optimal network generalization and heightened accuracy (Lungu et al. 2016). From Figures 4b to 6b, the flattening of the training curve (blue line) for all algorithms as MSE converges towards zero indicated a minimized loss function and a well-trained network. Table 2 illustrated activation function outcomes in which purelin had the lowest simulation performance due to linear metadata articulation, while the nonlinear sigmoid functions (logsig, tansig) produced R^2 values greater than 90%.

Both sigmoidal functions were proficiently adapted to unstructured datasets. A 10-hidden-cell ANN system improved data classification, particularly with sigmoid transfer functions and the purelin SCGANN. The Purelin trigger mechanism had no discernible trend on LM and BR algorithms while varying the hidden cells. Overall, the 5-10-2 configuration of the BR tool performs well, with an R2 of 0.9973 and an MSE of 0.023.

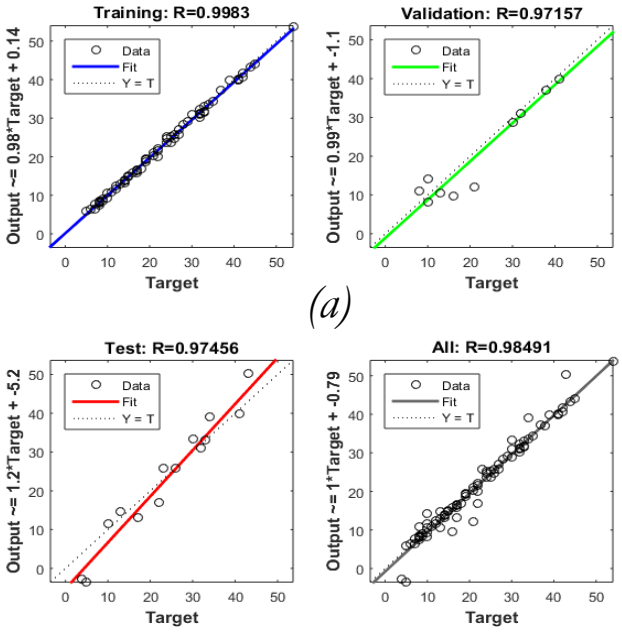

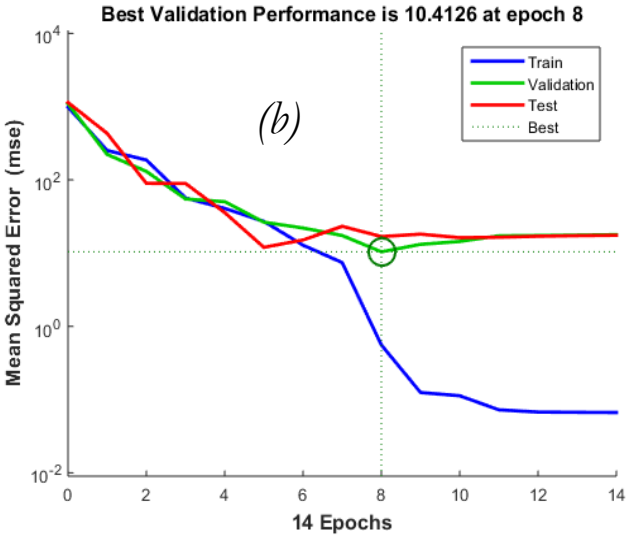

Figure 4. *LM (a) regression and (b) performance plots.*

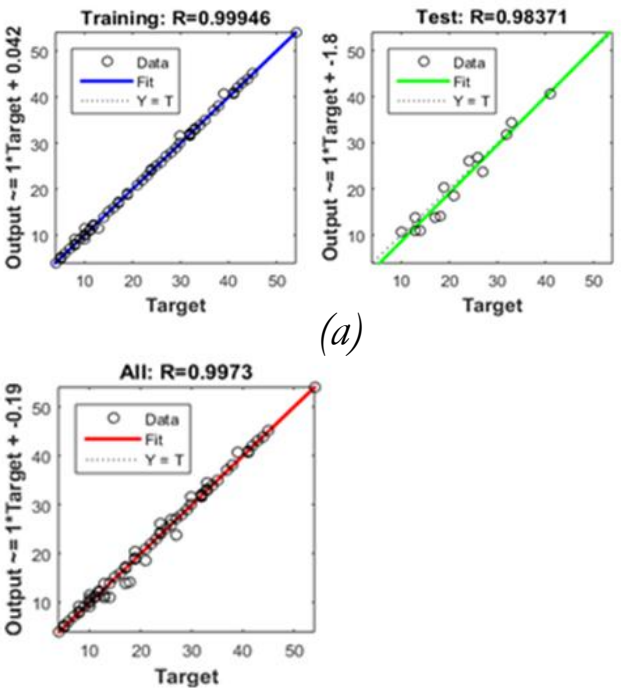

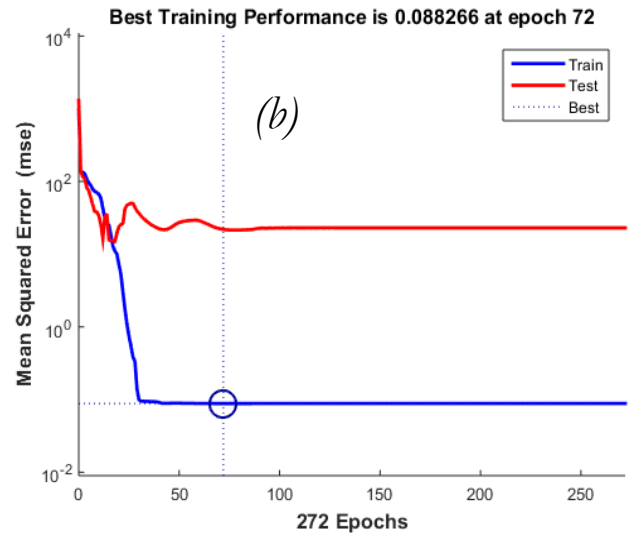

Figure 5. *BR (a) regression and (b) performance plots*

EQA 62 (2024): 45-54

DOI: 10.6092/issn.2281-4485/19040

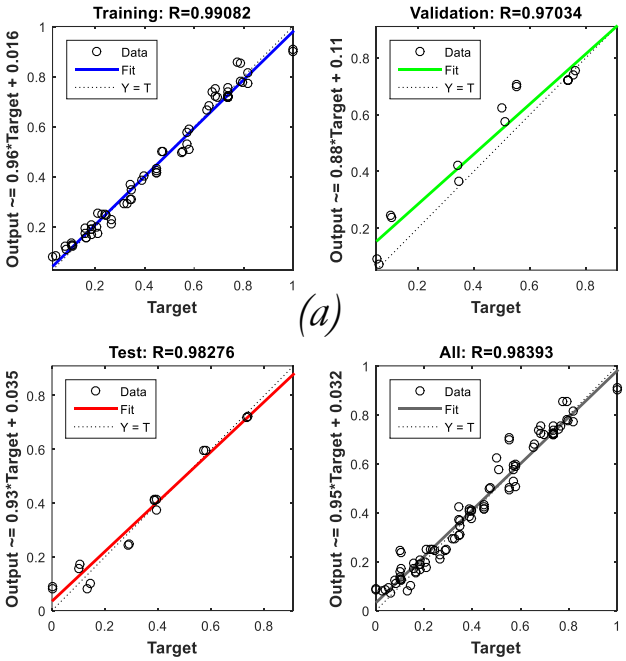

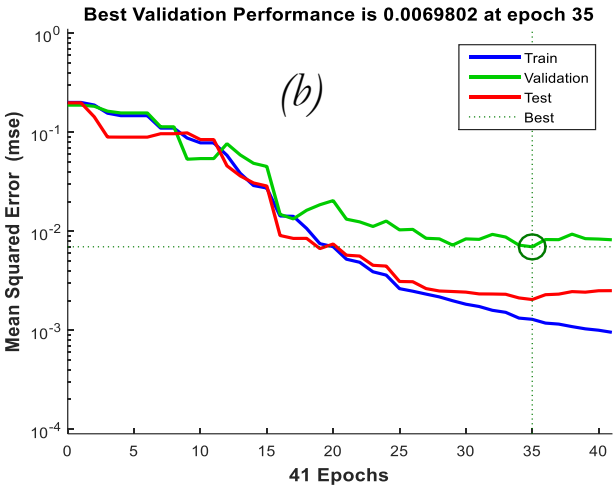

Figure 6. *SCG (a) regression and (b) performance plots.*

Function	Hidden layer nodes	LM		BR		SCG	
		R^2	MSE	R^2	MSE	R^2	MSE
Tansig	5-7-2	0.9698	0.234	0.9891	0.01	0.93424	0.00360
	5-8-2	0.9742	0.108	0.9787	0.101	0.96519	0.00269
	5-9-2	0.9390	0.028	0.9824	0.085	0.93416	0.00626
	5-10-2	0.9849	0.134	0.9973	0.023	0.98393	0.000954
Purelin	5-7-2	0.7480	66.4	0.7523	53.54	0.72963	0.0358
	5-8-2	0.7491	53.5376	0.7469	168.5	0.72563	0.0360
	5-9-2	0.7432	57.2	0.7454	60.6	0.73054	0.0240
	5-10-2	0.7433	56.6	0.7457	64.0	0.73173	0.0254
Logsig	5-7-2	0.9657	0.213	0.9902	0.180	0.95152	0.00335
	5-8-2	0.9790	0.212	0.9826	0.0948	0.94511	0.00598
	5-9-2	0.9812	0.107	0.9905	0.0964	0.96061	0.00264
	5-10-2	0.9831	0.182	0.9925	0.0022	0.96184	0.00368

Table 2
Neural network models with different activation functions and hidden neurons

ANFIS performance evaluation

The genfis1 and genfis2 FIS were trained with 5 input MFs ($3 \times 3 \times 3 \times 3 \times 3$ for GP and $16 \times 16 \times 16 \times 16 \times 16$ for SC) and 1 output MF. The grid partition model deployed 243 'IF-THEN' rules to compute and evaluate the estimated output, whereas the subtractive clustering model produced 16 rules. From Table 3, higher R^2 values were realized when the ANFIS model was optimized using the backpropagation (BP) method (0.8988-genfis1 and 0.8648-genfis2). The pi-shaped MF (pimf) in the backpropagation system developed a model that surpassed other models in forecasting outcomes (R^2 = 0.8988). The ANFIS loss function was calculated using the system RMSE for the training and testing data sets. Typically, the best deep-learning models exhibit the lowest RMSE values. According to the results in Table 3, the hybrid models demonstrated notably lower error levels throughout the training phase compared to the testing phase. In contrast,

DOI: 10.6092/issn.2281-4485/19040

Table 3. *ANFIS output*

Method	Optimization method	Membership function	Training RMSE	Testing RMSE	R^2
genfis1	Hybrid	trimf	2.0539e-06	0.15409	0.8344
		trapmf	1.11702e-06	0.22256	0.8429
		gaussmf	9.4275e-07	0.19824	0.8057
		gauss2mf	2.4686e-06	0.1467	0.8485
		gbellmf	1.3919e-06	0.19746	0.7967
		dsigmf	1.2887e-06	0.21076	0.8227
		pimf	1.03075e-06	0.20288	0.8112
	BP	trimf	0.79281	0.12675	0.8735
		trapmf	0.067224	0.141174	0.8693
		gaussmf	0.054787	0.16939	0.8447
		gauss2mf	0.055742	0.13981	0.8832
		gbellmf	0.07514	0.13652	0.8693
		dsigmf	0.057338	0.13985	0.8802
		pimf	0.051008	0.10418	0.8988
genfis2	Hybrid	gauss	1.2091e-06	0.18483	0.8547
	BP	gauss	0.011896	0.17765	0.8648

lation between the training and testing error values. The hybrid results suggested that the network was overfitting during the training stage. The optimization of the DFGD process can be observed via the rule reviewer system in Figure 7, which analyzed a series of 101 computed plots. At the specified optimal operating conditions, a sulfation reaction of 55.3% (Figure 7a) and a utilization response of 43.2% (Figure 7b) were obtained. These conditions include a diatomite to $Ca(OH)_2$ ratio of 0.375, a sorbent hydration time of 5 hours, a sorbent hydration temperature of 75 °C, an inlet gas concentration of 1500 ppm, and a desulfurization temperature of 140 °C. The artificial data differed from the measured values by 5.48% for sulfation and 4.32% for conversion.

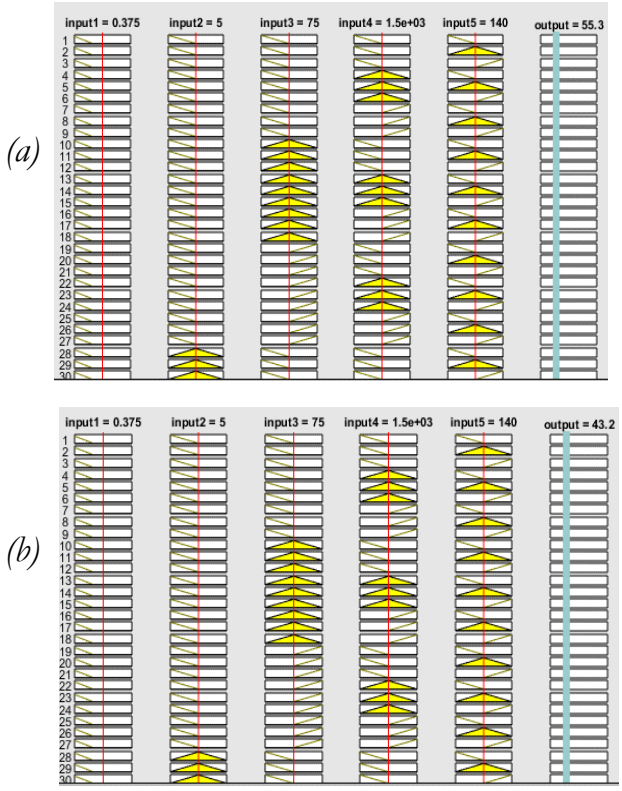

Figure 7 *ANFIS Optimized experimental conditions and responses for (a) SO_2 removal AND (b) sorbent conversion.*

Model comparison

The efficiency of the ANN and ANFIS predicting ability was explored using RMSE, MSE, and R^2 empirical comparison. All models achieved acceptable R^2 values emanating from successful training, learning, and reasoning. From Table 4, an analysis of the Y_1 estimations showed that the BR script had the strongest feature correlation (R^2 =

EQA 62 (2024): 45-54

DOI: 10.6092/issn.2281-4485/19040

0.9987), followed by LM (0.993) and SCG (0.9498), with ANFIS at 0.8898. For the Y_2 response, LM and BR attained an R^2 value of 0.9986, whereas SCG obtained the lowest R^2 of 0.9472. The fuzzy logic system, with an R^2 of 0.8927, was outperformed by all ANN models. Table 4 also revealed that SCG had a higher prediction accuracy from the lower RMSE (0.4178) and MSE (0.3371), supporting its reliability in perpetual estimation activities. This is consistent with an investigation by Baghirli (2015) of LM, BR, and SCG backpropagation classifiers, in which SCG produced the lowest mean absolute percentage error (MAPE) of 3.717 in wind speed projections (Baghirli 2015).

Table 4. *ANN and ANFIS performance comparison.*

Analysis	Sulfation efficiency (%)				Sorbent conversion (%)			
	LM	BR	SCG	ANFIS	LM	BR	SCG	ANFIS
RMSE	0.4847	0.4633	0.4178	0.7056	0.44971	0.368223	0.3371	0.5354
MSE	0.2349	0.2146	0.1745	0.4979	0.20299	0.135588	0.1136	0.2867
R^2	0.993	0.9987	0.9498	0.8988	0.9986	0.9986	0.9472	0.8927

Figures 8a and 8b provide graphical plots of values from the network-generated responses (Y_1 and Y_2) compared to the experimental data at random trial runs. The ANN systems presented high precision in forecasting functionality, illustrating that the training of the network was optimized. The ANFIS model had strong simulation capability during the initial runs (1 to 35), which diminished when mapping the testing data. This may be attributed to a scarcity of feed data, which hinders the ability to recognize patterns and effectively develop the desired decision-making process. (Keskin et al. 2006; Sada and Ikpeseni 2021). A comprehensive modeling study on hybrid algorithm data interpretation is underway to understand this problem and develop viable solutions.

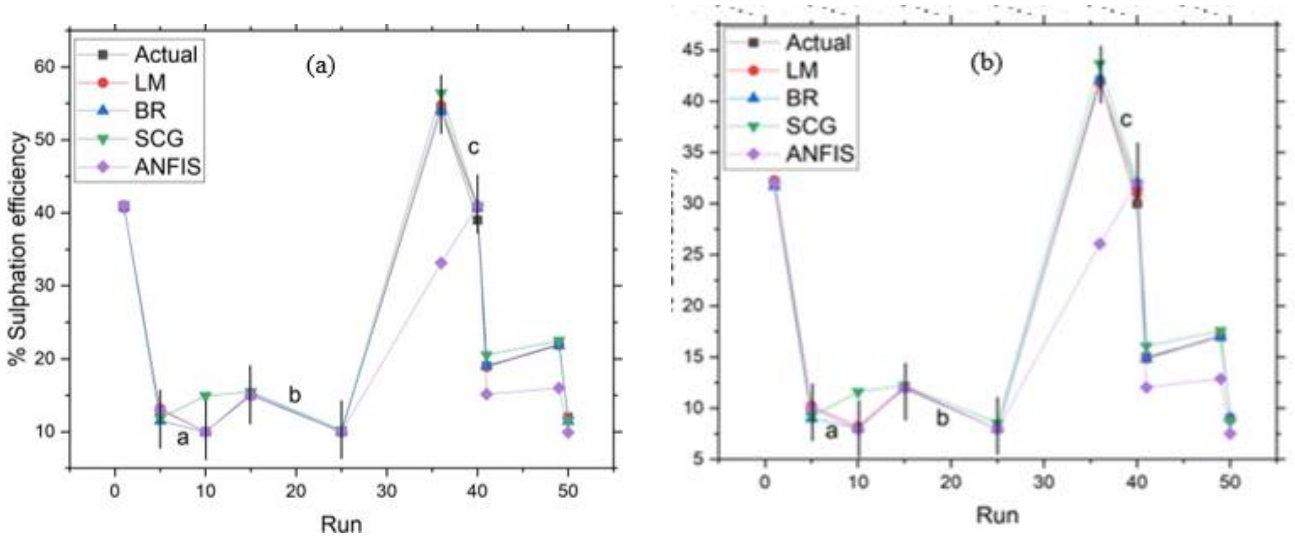

Figure 8. *Experimental vs synthetic data for (a) sulfation efficiency and (b) sorbent conversion*

Conclusion

Artificial intelligence (AI) is beneficial for comprehending continuous data systems and scientific processes, particularly in the domain of dry flue gas desulfurization (DFGD). This study used deep learning platforms to develop two prediction models, specifically artificial neural networks (ANN) and adaptive neuron-fuzzy inference systems (ANFIS). These networks were trained using various techniques to simulate SO_2 removal and sorbent consumption. The study confirmed the efficiency of

DOI: 10.6092/issn.2281-4485/19040

neural networks and fuzzy frameworks in DFGD adsorption measurements, with both models matching real data. BRANN had a higher correlation, whereas SCGANN generated lower error levels. The hyperbolic tangent activation function, in tandem with the 10 hidden node ANN design, produced ideal results. Conversely, the ANFIS system exhibited poor accuracy due to limited data, leading to inferior prediction. The hybrid method, which incorporated the grid partitioning ANFIS and pimf, produced desirable results for the fuzzy logic classifier. In general, the comparison of models showed that the ANN exhibited higher reliability and consistency in the analysis of DFGD.

References

BADILLO S., BANFAI B., BIRZELE F., DAVYDOV I.I., HUTCHINSON L., KAM-THONG T., SIEBOURG-POLSTER J., STEIERT B., ZHANG J.D. (2020) An Introduction to Machine Learning. Clinical pharmacology & therapeutics 107:871–885. https://doi.org/10.1002/cpt.1796

BAGHIRLI O. (2015) Comparison of Lavenberg-Marquardt, Scaled Conjugate Gradient and Bayesian Regularization Backpropagation Algorithms for Multistep Ahead Wind Speed Forecasting Using Multilayer Perceptron Feedforward Neural Network https://urn.kb.se/resolve?urn=urn%3Anbn%3Ase%3Auu%3Adiva-257086

BHATTI M.M., MARIN M., ZEESHAN A., ABDELSALAM S.I. (2020) Editorial: Recent Trends in Computational Fluid Dynamics. Frontiers in Physics 8. https://doi.org/10.3389/fphy.2020.593111

CARPENTER A.M. (2012) Low water FGD technologies. IEA Clean Coal Centre 73. ISBN 978-92-9029-530-3

CHAI T., DRAXLER R.R. (2014) Root mean square error (RMSE) or mean absolute error (MAE)? – Arguments against avoiding RMSE in the literature. Geoscientific model development 7:1247–1250. https://doi.org/10.5194/gmd-7-1247-2014

CHICCO D., WARRENS M.J., JURMAN G. (2021) The coefficient of determination R-squared is more informative than SMAPE, MAE, MAPE, MSE and RMSE in regression analysis evaluation. Peerj Computer Science 7:e623. https://doi.org/10.7717/peerj-cs.623

CHOPRA S., DHIMAN G., SHARMA A. (2021) Taxonomy of Adaptive Neuro-Fuzzy Inference System in Modern Engineering Sciences. Computational Intelligence and Neuroscience 2021:1–14. https://doi.org/10.1155/2021/6455592

EESA A.S., ARABO W.K. (2017) A Normalization Methods for Backpropagation: A Comparative Study. Science Journal of University of Zakho 5:319–323. https://doi.org/10.25271/2017.5.4.381

FATIMA F., FATIMA N., AMJAD T. (2020) 5. A review on acid rain: An environmental threat. Pure and Applied Biology (PAB) 10:301–310. ISSN 2304-2478

FU J., XIAO H., WANG T. (2019) Prediction Model of Desulfurization Efficiency of Coal-Fired Power Plants Based on Long Short-Term Memory Neural Network. In: 2019 International Conference on Internet of Things (iThings) and IEEE Green Computing and Communications (GreenCom) and IEEE Cyber, Physical and Social Computing (CPSCom) and IEEE Smart Data (SmartData). IEEE, Atlanta, GA, USA, pp 40–45. https://doi.org/10.1109/iThings/GreenCom/CPSCom/SmartData.2019.00030

GUO Y., XU Z., ZHENG C. (2019) Modeling and optimization of wet flue gas desulfurization system based on a hybrid modeling method. Journal of the Air & Waste Management Association 69:565–575. https://doi.org/10.1080/10962247.2018.1551252

HEAVISIDE C., WITHAM C., VARDOULAKIS S. (2021) Potential health impacts from sulphur dioxide and sulphate exposure in the UK resulting from an Icelandic effusive volcanic eruption. Science of the Total Environment 774:145549. https://doi.org/10.1016/j.scitotenv.2021.145549

JAKŠIĆ O., JAKŠIĆ Z., GUHA K. (2023) Comparing artificial neural network algorithms for prediction of higher heating value for different types of biomass. Soft Computing 27:5933–5950. https://doi.org/10.1007/s00500-022-07641-4

JAZAYERI K., JAZAYERI M., UYSAL S. (2016) Comparative Analysis of Levenberg-Marquardt and Bayesian Regularization Backpropagation Algorithms in Photovoltaic Power Estimation Using Artificial Neural Network. In: Perner P (ed) Advances in Data Mining. Applications and Theoretical Aspects. Springer International Publishing, Cham, pp 80–95. https://doi.org/10.1007/978-3-319-41561-1_7

KESKIN M.E., TAYLAN D., TERZI Ö. (2006) Adaptive neural-based fuzzy inference system (ANFIS) approach for modelling hydrological time series. Hydrological Sciences Journal 51:588–598. https://doi.org/10.1623/hysj.51.4.588

KONG Z., ZHANG Y., WANG X. (2020) Prediction and optimization of a desulphurization system using CMAC neural network and genetic algorithm. Journal of Environmental Engineering and Landscape Management 28:74–87. https://doi.org/10.3846/jeelm.2020.12098

DOI: 10.6092/issn.2281-4485/19040

LEROTHOLI L., EVERSON R.C., KOECH L. (2022) Semi-dry flue gas desulphurization in spray towers: a critical review of applicable models for computational fluid dynamics analysis. Clean Technologies and Environmental Policy 24:2011–2060. https://doi.org/10.1007/s10098-022-02308-y

LI X., HAN J., LIU Y. (2022) Summary of research progress on industrial flue gas desulfurization technology. Separation and Purification Technology 281:119849. https://doi.org/10.1016/j.seppur.2021.119849

LUNGU I., ADELA B., CARUTASU G. (2016) Prediction intelligent system in the field of renewable energies through neural networks. Economic Computation & Economic Cybernetics Studies & Research 50:85–102. ISSN: 0424-267X

MAKOMERE R., RUTTO H., KOECH L. (2023) The assessment of response surface methodology (RSM) and artificial neural network (ANN) modeling in dry flue gas desulfurization at low temperatures. Journal of Environmental Science and Health, Part A 58:191–203. https://doi.org/10.1080/10934529.2023.2174334

MAKOMERE R., RUTTO H., KOECH L., BANZA M. (2023) The use of artificial neural network (ANN) in dry flue gas desulphurization modelling: Levenberg–Marquardt (LM) and Bayesian regularization (BR) algorithm comparison. Canadian Journal of Chemical Engineering 101:3273–3286. https://doi.org/10.1002/cjce.24715

MAKOMERE R.S., RUTTO H.L., KOECH L. (2023) The Use of Cellulose Nanocrystals to Support Ca(OH)2 Nanoparticles with Diatomite Incorporation in Sulphur Capture at Low Temperatures: Optimisation and Modelling. Arabian Journal for Science and Engineering 48:8871–8885. https://doi.org/10.1007/s13369-022-07491-0

MANISALIDIS I., STAVROPOULOU E., STAVROPOULOS A., BEZIRTZOGLOU E. (2020) Environmental and Health Impacts of Air Pollution: A Review. Frontiers in Public Health 8. https://doi.org/10.3389/fpubh.2020.00014

ROY R.B., ROKONUZZAMAN M.d., AMIN N., MISHU M.K., ALAHAKOON S., RAHMAN S., MITHULANANTHAN N., RAHMAN K.S., SHAKERI M., PASUPULETI J. (2021) A Comparative Performance Analysis of ANN Algorithms for MPPT Energy Harvesting in Solar PV System. IEEE Access 9:102137–102152. https://doi.org/10.1109/ACCESS.2021.3096864

SADA S.O., IKPESENI S.C. (2021) Evaluation of ANN and ANFIS modeling ability in the prediction of AISI 1050 steel machining performance. Heliyon 7(2). https://doi.org/10.1016/j.heliyon.2021.e06136

SEPTIARINI T.W., MUSIKASUWAN S. (2018) Investigating the performance of ANFIS model to predict the hourly temperature in Pattani, Thailand. Journal of Physics: Conference Series 1097:012085. https://doi.org/10.1088/1742-6596/1097/1/012085

TRYGGVASON G. (2016) Chapter 6 - Computational Fluid Dynamics. In: KUNDU P.K., COHEN I.M., DOWLING D.R. (eds) Fluid Mechanics (Sixth Edition). Academic Press, Boston, pp 227–291. https://doi.org/10.1016/B978-0-12-405935-1.00006-X